Durga Prasad Chapagai, Jharna Tamang and Asit Saha*

Bifurcation Analysis for Small-Amplitude Nonlinear and Supernonlinear Ion-Acoustic Waves in a Superthermal Plasma

https://doi.org/10.1515/zna-2019-0210
Received June 20, 2019; accepted November 12, 2019; previously published online December 10, 2019

Abstract: Bifurcation analysis of small-amplitude nonlinear and supernonlinear periodic ion-acoustic waves (SNPIAWs) is reported in a three-constituent superthermal plasma composing of cold fluid ions and kappa-distributed electrons of two temperatures (cold and hot). Using the reductive perturbation technique, the plasma system is studied under the Korteweg-de Vries (KdV) and the modified KdV (mKdV) equations. Furthermore, the KdV and mKdV equations are transformed into planar dynamical systems applying travelling wave transfiguration. Possible qualitative phase profiles for the corresponding dynamical systems controlled by system parameters (κ, α_c, α_h and f) are shown. Small-amplitude SNPIAW solution for the mKdV equation is presented for the first time. Small-amplitude nonlinear periodic ion-acoustic wave (NPIAW) and ion-acoustic solitary wave solutions (IASWS) for both the KdV and mKdV equations are obtained. Effects of parameters κ and α_h on IASW, NPIAW and SNPIAW solutions are investigated.

Keywords: Dynamical System; KdV Equation; Modified KdV Equation; Reductive Perturbation Technique (RPT); Small-Amplitude Supernonlinear Wave.

1 Introduction

A newly discovered class of waves known as supernonlinear waves (SNWs), defined by the nontrivial topology of their phase portraits, was introduced by Dubinov and Kolotkov [1]. SNWs exist in plasma systems composing with at least three different plasma components. Phase portrait profiles are complex for plasma systems having more than three different components and result in more interesting wave structures, such as SNWs. Trajectories corresponding to such waves are evolved by number of fixed points and separatrix present in phase plots. Hence, any phase plot of SNWs consists of multiple periodic waves in continuous form of nested phase trajectories without selfintersection [2]. Dubinov and Kolotkov experimentally studied ion-acoustic waves (IAWs) in SF6-Ar plasma [3] and ion-acoustic supersolitons [4]. Verheest [5] studied nonlinear acoustic waves in nonthermal plasmas composed of positive and negative dusts. Baluku et al. [6] examined ion-acoustic solitary wave solutions (IASWS) in plasmas composed of two different temperature electrons. Researchers [7–13] showed their huge interest in studying SNWs. Verheest et al. [11] investigated ion-acoustic supersolitons in multicomponent plasmas composing cold fluid ions, kappa (κ)-distributed cold and hot electrons. Verheest et al. [14] confirmed the presence of supersolitons in plasma systems having at least three types of particles. Olivier et al. [15] reported the influences of collision in SNWs. Ali et al. [16] studied SNWs under Sharma-Tasso-Olver equation and obtained exact solutions. Dubinov and Kolotkov [17] reported SNWs in astrophysical and laboratory environments. Kamalam and Ghosh [18] reported supersolitons in magnetised plasmas for low frequency waves.

Reductive perturbation technique (RPT) plays a significant part in the study of small-amplitude nonlinear waves. Mathematically, RPT redefines space and timescale [19] in fundamental model equations of systems that describe long wavelength situation. Using RPT, model equations are deduced to nonlinear evolution equations, such as, the Korteweg-de Vries (KdV) equation, the Burgers equation, etc. Many researchers [20–26] studied nonlinear acoustic wave features implementing RPT. Hence, it is important to note that RPT may be applied in the study of small-amplitude SPWs in plasmas.

Over the decades, the study on plasma systems composed of long-range correlations, was acknowledged by highly energetic electrons detected in plasmas near Earth,

***Corresponding author: Asit Saha,** Department of Mathematics, Sikkim Manipal Institute of Technology, Sikkim Manipal University, Majitar, Rangpo, East Sikkim 737136, India, E-mail: asit_saha123@rediffmail.com, asit.s@smit.smu.edu.in. https://orcid.org/0000-0001-7542-7699
Durga Prasad Chapagai and Jharna Tamang: Department of Mathematics, Sikkim Manipal Institute of Technology, Sikkim Manipal University, Majitar, Rangpo, East Sikkim 737136, India, E-mail: durgachapagai522@gmail.com (D.P. Chapagai); jharnatamang.12@gmail.com, Jharna_201710008@smit.smu.edu.in. https://orcid.org/0000-0002-4447-3024 (J. Tamang)

containing complex shapes of lengthy tails that vigorously drift away to the non-Maxwellian distribution. In 1955, Renyi [27] introduced an alternative perspective defined as κ-distribution. The distribution (κ) is convenient to examine active modelling of waves and instabilities in space plasmas. This distribution extends righteous substitute of the Maxwell distribution for portraying systems like space plasmas. κ-distribution at high velocities obeys the law of inverse power [28]

$$f_\kappa(v) = \frac{n_0}{(\pi\kappa\theta^2)^{3/2}} \frac{\Gamma(\kappa+1)}{\Gamma(\kappa-1/2)} \left(1 + \frac{v^2}{\kappa\theta^2}\right),^{-(\kappa+1)} \quad (1)$$

where $v = v^2x + v^2y + v^2z$,θ stands for effective thermal speed $v_{\rm th} = \left(\frac{2K_BT}{m}\right)^{\frac{1}{2}}$ given by $\theta^2 = \left(\frac{\kappa-\frac{3}{2}}{\kappa}\right)v_{\rm th}^2$ and κ stands for spectral index, which measure strength of superthermal elements [29, 30]. Thus, from (1), the normalised electron number density is

$$n_e = \left(1 - \frac{\phi}{\kappa - 3/2}\right)^{-\kappa+\frac{1}{2}}. \quad (2)$$

This velocity distribution behaves like Maxwellian, as $\kappa \to \infty$. Saini et al. [31] reported the characteristics of IAWs in cold ions with kappa (κ)-distributed electrons. Baluku and Hellberg [32] reported solitary waves and double layers of dust-acoustic waves in systems having κ-distributed electrons and ions. Ahmadihojatabad et al. [33] studied the effects of superthermal electrons in plasmas under magnetic effect. Sahu [34] expanded the study of EAWs in superthermal plasmas. Recently, many researchers [35–38] studied nonlinear acoustic waves in different plasma systems consisting of superthermal electrons. Applications of κ-distribution are extensively found in data examination of spacecraft observation on magnetospheric plasma sheet of Earth, Jupiter [35], etc.

Bifurcation is the change in qualitative structure of flow in dynamical system due to variation in dynamic parameters of plasma system [39]. Bifurcations are very significant in dynamical systems as systems are allowed for transitions and instabilities when some controlled parameters of the systems are varied. Samanta et al. [40] evaluated bifurcation of nonlinear travelling waves in plasmas employing RPT for the first time. Some works [10, 41–43] were reported on arbitrary amplitude supersolitons of IAWs in multiconstituent plasmas. References [44, 45] reported examination of nonlinear acoustic waves in superthermal plasmas applying bifurcations in different plasma systems. Saha and Tamang [46] presented arbitrary amplitude supernonlinear periodic ion-acoustic waves (SNPIAWs) by implementing bifurcation analysis through direct approach. Very recently, Tamang and Saha [47] and Prasad et al. [48] reported existence of arbitrary amplitude SPWs using the concept of bifurcation theory. Applying RPT, Verheest et al. [49] suggested existence of superacoustic modified KdV (mKdV) solitons. However, bifurcations of small-amplitude SNPIAWs have not been reported theoretically in nonlinear plasma system which consists of cold and hot temperature κ-distributed electrons to the best of our knowledge. Plasmas composed of simultaneous cold and hot electrons were reported experimentally [50, 51]. Therefore, the main aim of our work is to examine existence of small-amplitude SNPIAWs in superthermal plasma system implementing bifurcation analysis of dynamical systems [52–54]. For this purpose, we investigate IAWs in frameworks of the KdV and mKdV equations employing RPT in a three-component plasma system.

This work is arranged as: In section 2, fundamental equations are considered. In section 3, derivations of the KdV and mKdV equations are done. In section 4, dynamical system of the KdV equation is formed. In section 5, dynamical system of the mKdV equation is obtained. In section 6, solutions for the KdV and mKdV equations are obtained, and section 7 is for conclusions.

2 Fundamental Equations

We examine small-amplitude IAWs in a three-constituent plasma system constituting of cold fluid ions and κ-distributed different temperature (hot and cold) electrons. Propagation of IAWs is governed by fundamental equations [49]:

$$\frac{\partial n}{\partial t} + \frac{\partial}{\partial x}(nu) = 0, \quad (3)$$

$$\frac{\partial u}{\partial t} + u\frac{\partial u}{\partial x} = -\frac{\partial \phi}{\partial x}, \quad (4)$$

$$\frac{\partial^2\phi}{\partial x^2} = f\left(1 - \frac{\alpha_c\phi}{\kappa-\frac{3}{2}}\right)^{-\kappa+\frac{1}{2}} + (1-f)\left(1 - \frac{\alpha_h\phi}{\kappa-\frac{3}{2}}\right)^{-\kappa+\frac{1}{2}} - n, \quad (5)$$

where n, u, ϕ and f are, respectively, number density of cold ions, velocity of ions, electrostatic potential and fractional charge density of cold electrons. $\alpha_c = \frac{T_{\rm eff}}{T_c}$ and $\alpha_h = \frac{T_{\rm eff}}{T_h}$, where $T_{\rm eff} = \frac{T_cT_h}{fT_h+(1-f)T_c}$ is effective temperature with hot and cold electron temperatures T_h and T_c, respectively [50].

The considered plasma system is normalised by: n_0 normalises n, $C_s = \left(\frac{k_BT_e}{m}\right)^{\frac{1}{2}}$ normalises u, where k_B denotes the Boltzmann constant, m stands for ion mass, and e denotes strength of electron charge. $\frac{k_B T_e}{e}$ normalises ϕ, $\omega^{-1} = \left(\frac{m}{4\pi n_0 e^2}\right)^{\frac{1}{2}}$ normalises t, where ω stands for frequency of plasma and the Debye length $\lambda_D = \left(\frac{k_B T_e}{4\pi n_0 e^2}\right)^{\frac{1}{2}}$ normalises x.

3 Derivations of the KdV and mKdV Equations

To derive the KdV and mKdV equations, we consider following stretching by using RPT

$$\xi = \varepsilon^{\frac{1}{2}}(x - vt) \quad \text{and} \quad \tau = \varepsilon^{\frac{3}{2}} t, \tag{6}$$

where ε measures weakness of nonlinearity and v denotes phase velocity of IAWs. Let us consider expansions for dependent variables:

$$\begin{cases} n = 1 + \varepsilon n_1 + \varepsilon^2 n_2 + \varepsilon^3 n_3 \ldots \\ u = 0 + \varepsilon u_1 + \varepsilon^2 u_2 + \varepsilon^3 u_3 \ldots \\ \phi = 0 + \varepsilon \phi_1 + \varepsilon^2 \phi_2 + \varepsilon^3 \phi_3 \ldots . \end{cases} \tag{7}$$

Substituting (6), (7) in fundamental (3)–(5), one can obtain following relations by comparing the coefficients of $\varepsilon^{3/2}$

$$n_1 = \frac{1}{v} u_1, u_1 = \frac{1}{v} \phi_1, \tag{8}$$

$$v^2 = \frac{1}{a(f\alpha_c + (1-f)\alpha_h)}, \tag{9}$$

where $a = \frac{\kappa - \frac{1}{2}}{\kappa - \frac{3}{2}}$. By comparing the coefficients of $\varepsilon^{5/2}$, following equations are obtained

$$\frac{\partial n_1}{\partial \tau} - v \frac{\partial n_2}{\partial \xi} + \frac{\partial}{\partial \xi}(n_1 u_1) + \frac{\partial}{\partial \xi} u_2 = 0, \tag{10}$$

$$\frac{\partial u_1}{\partial \tau} - v \frac{\partial u_2}{\partial \xi} + u_1 \frac{\partial u_1}{\partial \xi} + \frac{\partial \phi_2}{\partial \xi} = 0, \tag{11}$$

$$\frac{\partial^2 \phi_1}{\partial \xi^2} + n_2 - a\phi_2(f\alpha_c + (1-f)\alpha_h) - b\phi_1^2(f\alpha_c^2 + (1-f)\alpha_h^2) = 0, \tag{12}$$

where $b = \frac{\kappa^2 - \frac{1}{4}}{2\left(\kappa - \frac{3}{2}\right)^2}$. Differentiating (12) w.r. to ξ and eliminating all higher order perturbed terms using (8)–(11), we derive the required KdV equation as

$$\frac{\partial \phi_1}{\partial \tau} + A\phi_1 \frac{\partial \phi_1}{\partial \xi} + B \frac{\partial^3 \phi_1}{\partial \xi^3} = 0, \tag{13}$$

where $A = \frac{v^3}{2}\left(\frac{3}{v^4} - 2b(f\alpha_c^2 + (1-f)\alpha_h^2)\right)$ and $B = \frac{v^3}{2}$.

Here, we observe numerically that for certain critical values such as, $\kappa = 4.7866$, $\alpha_c = 1.1$, $\alpha_h = 0.09$ and $f = 0.2522$, nonlinear coefficient A of the KdV equation vanishes. For such set of values, the KdV equation is not valid. Therefore, we derive the mKdV equation for IAWs considering following stretching

$$\xi = \varepsilon(x - vt) \quad \text{and} \quad \tau = \varepsilon^3 t. \tag{14}$$

Substituting (7) and (14) in fundamental (3)–(5), we obtain following equations comparing the coefficients of ε^2,

$$n_2 = a\phi_2(f\alpha_c + (1-f)\alpha_h) - b\phi_2^2(f\alpha_c^2 + (1-f)\alpha_h^2), \tag{15}$$

$$u_2 = \frac{1}{v}\left(\frac{\phi_1^2}{2v^2} + \phi_2\right). \tag{16}$$

We also obtain following equations comparing the coefficients of ε^4,

$$-v\frac{\partial n_3}{\partial \xi} + \frac{\partial n_1}{\partial \tau} + \frac{\partial}{\partial \xi}(n_1 u_2 + n_2 u_1 + u_3) = 0 \tag{17}$$

$$-v\frac{\partial u_3}{\partial \xi} + \frac{\partial u_1}{\partial \tau} + \frac{\partial}{\partial \xi}(u_1 u_2) + \frac{\partial \phi_3}{\partial \xi} = 0 \tag{18}$$

$$\begin{aligned} &\frac{\partial^2 \phi_1}{\partial \xi^2} + n_3 - a(f\alpha_c + (1-f)\alpha_h)\phi_3 \\ &\quad - 2b\big(f\alpha_c^2 + (1-f)\alpha_h^2\big)(\phi_1\phi_2) \\ &\quad - c\big(f\alpha_c^3 + (1-f)\alpha_h^3\big)\phi_1^3 = 0. \end{aligned} \tag{19}$$

Differentiating (19) with respect to ϕ_1, removing all higher order perturbed terms using (15)–(18) and proceeding in similar way as in case of the KdV equation, we get the modified KdV (mKdV) equation

$$\frac{\partial \phi_1}{\partial \tau} + C\phi_1^2 \frac{\partial \phi_1}{\partial \xi} + B \frac{\partial^3 \phi_1}{\partial \xi^3} = 0, \tag{20}$$

where $C = \frac{v^3}{2}\left(\frac{3}{v^6} + \frac{3}{v^2} b(f\alpha_c^2 + (1-f)\alpha_h^2) - 3c(f\alpha_c^3 + (1-f)\alpha_h^3)\right)$ and $c = \frac{(\kappa^2 - \frac{1}{4})(\kappa + \frac{3}{2})}{6(\kappa - \frac{3}{2})^3}$.

4 Formation of Dynamical System for the KdV Equation

Let us consider $\chi = \xi - V\tau$ as travelling wave transformation, where speed of travelling wave is denoted by V; (13) becomes

$$-V\frac{d\phi_1}{d\chi} + A\phi_1 \frac{d\phi_1}{d\chi} + B\frac{d^3\phi_1}{d\chi^3} = 0. \tag{21}$$

Integrating (13) w.r.t. to χ and using conditions $\phi_1 \to 0$, $\frac{d\phi_1}{d\chi} \to 0$, $\frac{d\phi_1}{d\chi} \to 0$ as $\chi \pm \infty$, we get

$$\frac{d^2\phi_1}{d\chi^2} = \frac{1}{B}\left(V\phi_1 - \frac{A}{2}\phi_1^2\right). \tag{22}$$

Then, (22) is presented in form of dynamical system as:

$$\begin{cases} \dfrac{d\Phi}{d\chi} = z, \\ \dfrac{dz}{d\chi} = \dfrac{1}{B}\left(V\Phi - \dfrac{A}{2}\Phi^2\right), \end{cases} \tag{23}$$

where we put $\Phi = \phi_1$ for simplicity.

4.1 Phase Plane Analysis

Mathematically, bifurcation in dynamical systems [39] is a significant change in system due to variation in physical parameter of the system. Phase plane analysis using bifurcation theory gives underlying feature of dynamical systems. It is reported that any qualitative orbit in phase plane corresponds to solution of travelling wave [46]. Considering the bifurcation analysis of dynamical systems, qualitative phase portraits are presented for system (23) with parameters κ, f, α_c and α_h. Fixed points of the system (23) are obtained by solving following equations simultaneously

$$\frac{d\Phi}{d\chi} = 0 \text{ and } \frac{dz}{d\chi} = 0,$$

which imply

$$z = 0 \text{ and } \Phi\frac{1}{B}\left(V - \frac{A}{2}\Phi\right) = 0,$$

$$\Rightarrow z = 0 \text{ and } \Phi = 0, \frac{2V}{A}.$$

It is clear that the system (23) has two fixed points $E_0(\Phi_0, 0)$ and $E_1(\Phi_1, 0)$, where $\Phi_0 = 0$ and $\Phi_1 = \frac{2V}{A}$. The Jacobian matrix J for any system

$$\begin{cases} \dfrac{d\Phi}{d\chi} = f(\Phi, z), \\ \dfrac{dz}{d\chi} = g(\Phi, z), \end{cases}$$

is given by

$$J = \begin{pmatrix} \dfrac{\partial f(\Phi, z)}{\partial \Phi} & \dfrac{\partial f(\Phi, z)}{\partial z} \\ \dfrac{\partial g(\Phi, z)}{\partial \Phi} & \dfrac{\partial g(\Phi, z)}{\partial z} \end{pmatrix}. \tag{24}$$

Using (24), the Jacobian matrix of the system (23) is

$$J = \begin{pmatrix} 0 & 1 \\ \dfrac{1}{B}(V - A\Phi_i) & 0 \end{pmatrix},$$

and determinant of J is expressed by M as

$$M = \det J(\Phi_i, 0) = -\frac{1}{B}(V - A\Phi_i),$$

where $i = 0, 1$. If $M < 0$, then fixed point $E_i(\Phi_i, 0)$ is a saddle node and for $M > 0$, fixed point $E_i(\Phi_i, 0)$ is a centre [39]. With support of numerical computations, we display qualitative phase portrait profiles in Figures 1 and 2 for the system (23) relying on system parameters κ and α_h with definite values of α_c, f and V.

In Figure 1, we display phase portrait profile for the KdV (13) for $\kappa = 1.6, \alpha_h = 0.1, \alpha_c = 1.1, f = 0.1$, and $V = 0.9$. It is observed that there exists saddle point at $E_0(0, 0)$ and centre at $E_1(\phi_1, 0)$. A nonlinear homoclinic orbit ($NHO_{1,0}$) about $E_0(0, 0)$ enclosing fixed point $E_1(\phi_1, 0)$ and nonlinear periodic orbit ($NPO_{1,0}$) enclosing fixed point $E_1(\phi_1, 0)$ correspond to IASW and nonlinear periodic ion-acoustic wave (NPIAW) solutions, respectively.

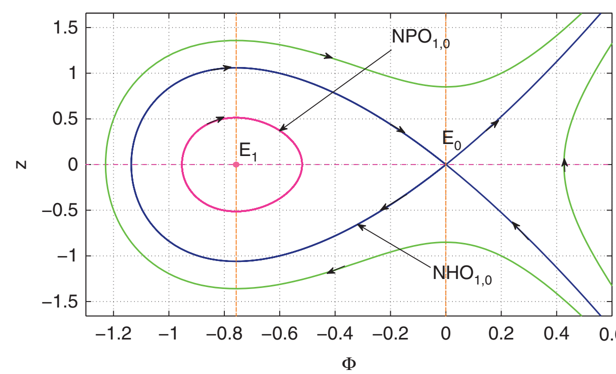

Figure 1: Phase portrait of dynamical system (23) with $\kappa = 1.6$, $\alpha_h = 0.1$, $\alpha_c = 1.1$, $f = 0.1$, and $V = 0.9$.

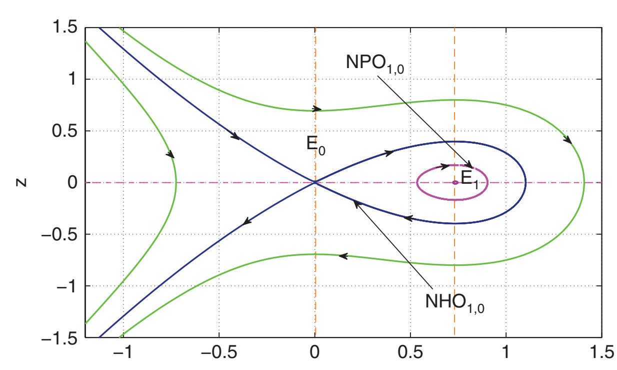

Figure 2: Phase portrait of dynamical system (23) for $\kappa = 1.7$, $\alpha_h = 0.3$, $\alpha_c = 1.1$, $f = 0.01$ and $V = 0.2$.

Similarly, in Figure 2, we obtain phase portrait profile for the KdV (13) with $\kappa = 1.7$, $\alpha_h = 0.3$, $\alpha_c = 1.1$, $f = 0.01$ and $V = 0.2$. $NHO_{1,0}$ about $E_0(0,0)$ enclosing fixed point $E_1(\phi_1, 0)$ corresponds to IASW solution and $NPO_{1,0}$ enclosing fixed point $E_1(\phi_1, 0)$ corresponds to NPIAW solution.

5 Formation of Dynamical System for the mKdV Equation

Similarly, using same transformation as in case of the KdV (13) in (20), we obtain

$$\frac{d^2\phi_1}{d\chi^2} = \frac{1}{B}\left(V\phi_1 - \frac{C}{3}\phi_1^3\right). \tag{25}$$

Let us put $\Phi = \phi_1$. (25) is equivalent to

$$\begin{cases} \dfrac{d\Phi}{d\chi} = z, \\ \dfrac{dz}{d\chi} = \dfrac{1}{B}\left(V\Phi - \dfrac{C}{3}\Phi^3\right). \end{cases} \tag{26}$$

5.1 Phase Plane Analysis

From Figures 1 and 2, it is evident that IASWs and NPIAWs are possible for the KdV (13). Now, we present phase portrait profile of system (26) for the mKdV (20) with fixed values of κ, α_h, α_c, f and V. For that purpose, fixed points of the system (26) are obtained by solving following equations simultaneously

$$\frac{d\Phi}{d\chi} = 0 \text{ and } \frac{dz}{d\chi} = 0,$$

which imply

$$z = 0 \text{ and } \Phi\frac{1}{B}\left(V - \frac{C}{3}\Phi^2\right) = 0,$$

$$\Rightarrow z = 0 \text{ and } \Phi = 0, \pm\sqrt{\frac{3V}{C}}.$$

Therefore, there are three fixed points $E_0(\Phi_0, 0)$, $E_1(\Phi_1, 0)$ and $E_2(\Phi_2, 0)$ of the system (26), where

$$\Phi_0 = 0, \Phi_1 = \sqrt{\frac{3V}{C}}, \text{ and } \Phi_2 = -\sqrt{\frac{3V}{C}}.$$

Using (24), the Jacobian matrix J for the system (26) is

$$J = \begin{pmatrix} 0 & 1 \\ \frac{1}{B}(V - C\Phi_i^2) & 0 \end{pmatrix},$$

and determinant of J is expressed by

$$M = \det J(\Phi_i, 0) = -\frac{1}{B}(V - C\Phi_i^2),$$

where $i = 0, 1, 2$. If $M < 0$, then fixed point $E_i(\Phi_i, 0)$ is a saddle node and for $M > 0$, fixed point $E_i(\Phi_i, 0)$ is a centre [39]. Applying the phase plane analysis of dynamical systems [52–54], we plot phase portrait profile in Φ-z plane in Figure 3.

Through computation, we show phase portrait profile of (26) for the mKdV (20) relying on system parameters κ, α_h, α_c, f and V in Figure 3. We observe a couple of $NHO_{1,0}$ enclosing one fixed point and no separatrix. Any qualitative orbits in phase plane profile correspond to a travelling wave solution. Here, $NHO_{1,0}$ enclosing fixed point E_1 corresponds to rarefactive IASWs. Similarly, $NHO_{1,0}$ enclosing fixed point E_2 corresponds to compressive IASWs. $NPO_{1,0}$ around E_1 and E_2 correspond to NPIAW solutions. There also exists a class of supernonlinear periodic orbit ($SPO_{3,1}$) enclosing fixed points E_0, E_1 and E_2 with one separatrix. $SPO_{3,1}$ corresponds to SNPIAW solution of the mKdV (20). It is observed numerically that small-amplitude SNPIAW features for the mKdV (20) exist in the considered plasma system for range $\kappa \geqslant 2.6$ keeping other parameters fixed as $\alpha_h = 0.1$, $\alpha_c = 1.1$, $f = 0.1$ and $V = 0.2$. Also, it is interesting to obtain small-amplitude SNPIAW features in the range $0 < \alpha_h \leqslant 0.17$ with other parameters fixed as $\kappa = 3$, $\alpha_c = 1.1$, $f = 0.1$ and $V = 0.2$.

6 Ion-Acoustic Wave Solutions

We encountered existence of IASWS for the KdV and mKdV equations from their respective phase profiles Figures 1–3. Therefore, analytical IASW solutions for the KdV and mKdV equations are obtained as:

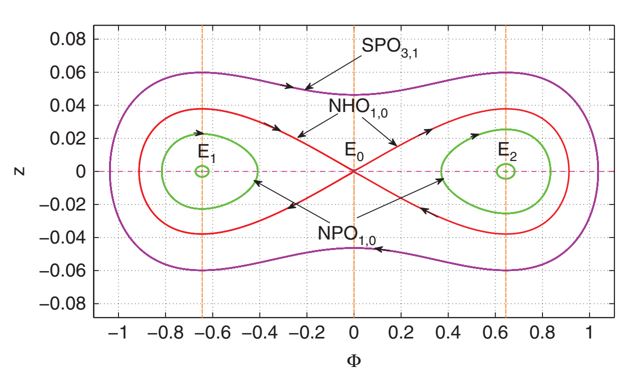

Figure 3: Phase portrait of dynamical system (26) for $\kappa = 3$, $\alpha_h = 0.1$, $\alpha_c = 1.1$, $f = 0.1$ and $V = 0.2$.

The KdV (13) supports IASWS given by:

$$\Phi = \frac{3P}{2S}\operatorname{sech}^2\left(\sqrt{\frac{P}{4}}\chi\right), \tag{27}$$

where $P = \frac{(\kappa-\frac{1}{2})}{(\kappa-\frac{3}{2})}(f\alpha_c + (1-f)\alpha_h) - \frac{1}{V^2}, S = \frac{3}{2V^4} - \frac{(\kappa^2-\frac{1}{4})}{2(\kappa-\frac{3}{2})^2}(f\alpha_c^2 + (1-f)\alpha_h^2)$, where amplitude is $\frac{3P}{2S}$ and width is $\sqrt{\frac{4}{P}}$.

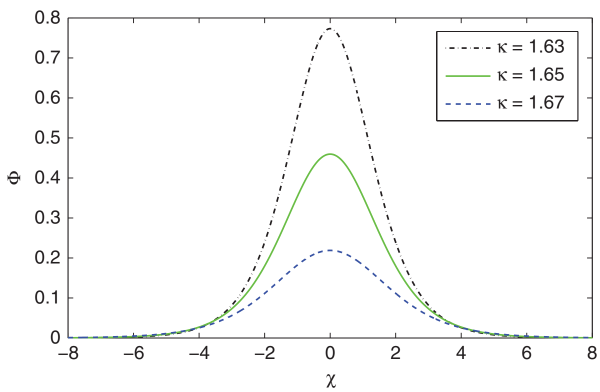

Figure 4: Ion-acoustic solitary wave solution (IASWS) of the Korteweg-de Vries (KdV) (13) for different values of κ with $\alpha_h = 0.1, \alpha_c = 1.1, f = 0.1$ and $V = 0.9$.

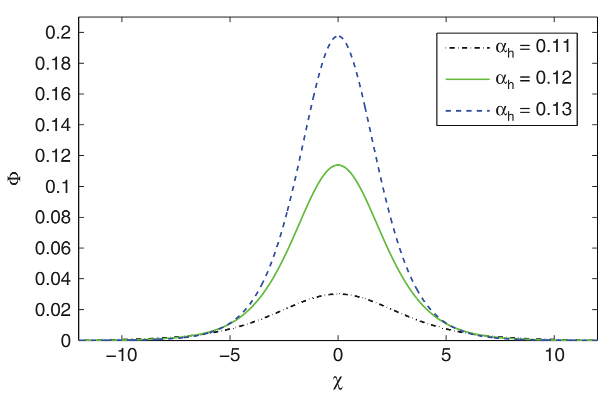

Figure 5: IASWS of the KdV (13) for distinct values of α_h with $\kappa = 1.7, \alpha_c = 1.1, f = 0.1$ and $V = 0.9$.

Similarly, the mKdV (20) supports both compressive and rarefactive IASWS:

$$\Phi = \pm\sqrt{\frac{6V}{C}}\operatorname{sech}\left(\sqrt{\frac{V}{B}}\chi\right), \tag{28}$$

where amplitude and width are given by $\sqrt{\frac{6V}{C}}$ and $\sqrt{\frac{B}{V}}$, respectively. By numerical analysis, we show effects of κ and α_h on IASWS of (13) and (20).

In Figure 4, we present change in IASWS of the KdV (13) with discrete values of κ and system parameters as $\alpha_h = 0.1, \alpha_c = 1.1, f = 0.1$ and $V = 0.9$. From Figure 4, it is evident that when electrons evolve far away from Maxwellian, IASWS become spiky. As a result, increase in spectral index (κ) of electrons shows decrease in amplitude and increase in width of IASWS.

In Figure 5, variation on IASWS of the KdV (13) for distinct values of α_h with $\kappa = 1.7, \alpha_c = 1.1, f = 0.1$ and $V = 0.9$ is shown. It is observed that when temperature of hot electrons increases, correspondingly ratio α_h of effective temperature and hot electron temperature decreases and this results in decreasing of amplitude and increasing of width of IAW. As a result, IASW becomes smooth.

We show effects of κ in Figure 6a and α_h in Figure 6b on NPIAW of the KdV (13). When spectral index (κ) of electrons is increased, amplitude and width of NPIAW are enhanced. On the other hand, when temperature of hot electrons is increased, the ratio α_h of effective temperature and hot electron temperature becomes relatively low, as a result both amplitude and width of NPIAW dwindle.

In Figure 7, changes in compressive and rarefactive IASWS of the mKdV (20) for distinct value of κ with other parameters $\alpha_h = 0.1, \alpha_c = 1.1, f = 0.1$ and $V = 0.2$ are shown. Here Figure 7 shows decrease in amplitude and width of both compressive and rarefactive IASWS when spectral index κ of electrons is approaching to Maxwellian limit.

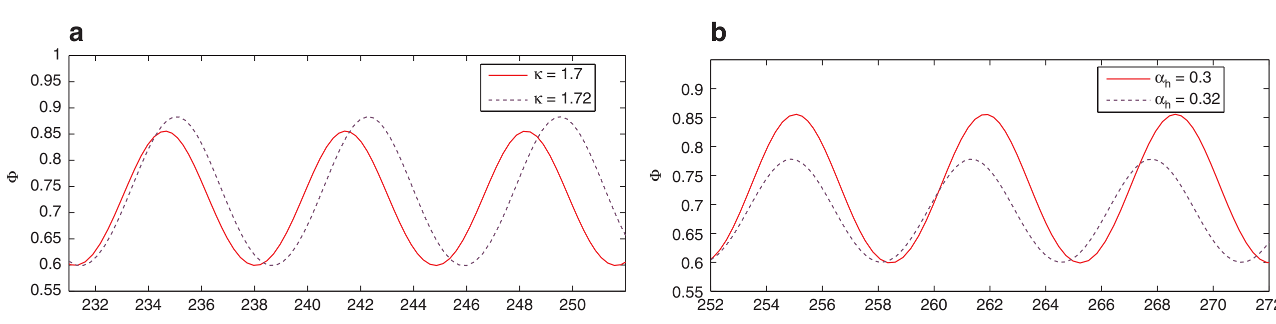

Figure 6: Nonlinear periodic ionacoustic wave (NPIAW) solution of the KdV (13) for different values of κ in (a) and α_h in (b) with $\alpha_c = 1.1$, $f = 0.01$ and $V = 0.2$.

In Figure 8, we observe changes in compressive and rarefactive IASWS of the mKdV (20) for distinct values of α_h with fixed values of other parameters $\kappa = 3$, $\alpha_c = 1.1$, $f = 0.1$ and $V = 0.9$. In this case, low temperature of hot electrons enhances temperature ratio α_h, which results into increment of amplitude and decrease of width of both compressive and rarefactive IASWS of the mKdV (20).

We display effects of parameters κ and α_h on NPIAW for the mKdV (20) in Figure 9. When spectral index of electrons (κ) is approaching to Maxwell distribution, it is observed that both amplitude and width of NPIAW are decreasing (see Fig. 9a). However, in Figure 9b, we observe that with low temperature of hot electrons, NPIAW becomes more smooth.

It is interesting to observe different class of waves known as SNPIAW of small-amplitude for system (26) obtained from the mKdV (20). Small-amplitude SNPIAW solution for the mKdV (20) is obtained corresponding to $SPO_{3,1}$ presented in Figure 3. Variations of system parameters κ and α_h on small-amplitude SNPIAW of the mKdV (20) are shown in Figures 10 and 11.

$SPO_{3,1}$ present in Figure 3 corresponds to SNPIAW solution which is shown by Figure 10. We display the effect of κ on SNPIAW solution of the mKdV (20) in Figure 10

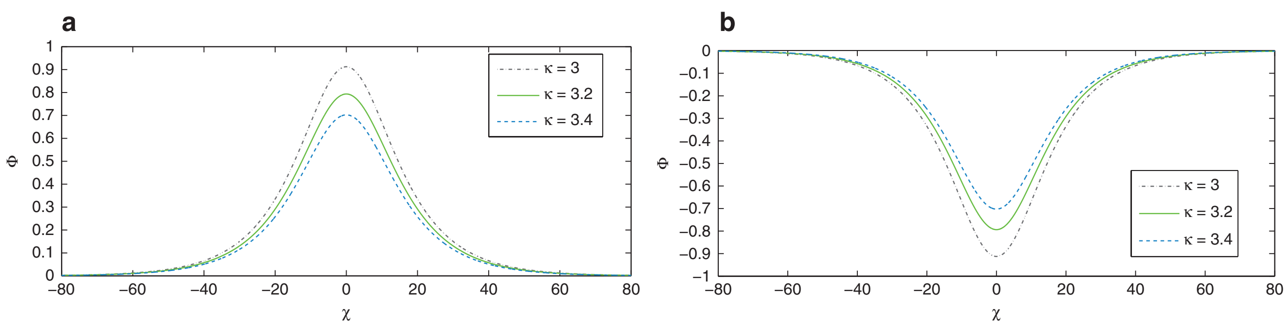

Figure 7: (a) Compressive and (b) rarefactive IASW solutions of the modified KdV (20) for distinct values of κ with $\alpha_h = 0.1$, $\alpha_c = 1.1$, $f = 0.1$ and $V = 0.2$.

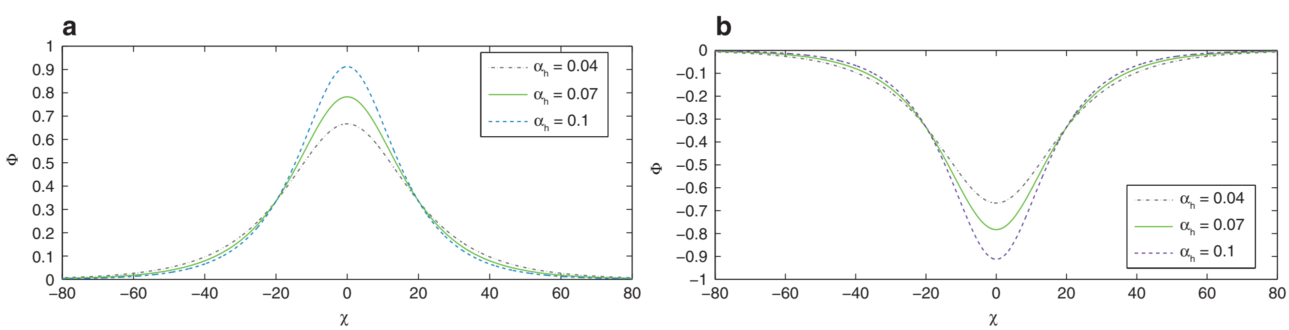

Figure 8: (a) Compressive and (b) rarefactive IASWS of the mKdV (20) for different α_h with $\kappa = 3$, $\alpha_c = 1.1$, $f = 0.1$ and $V = 0.2$.

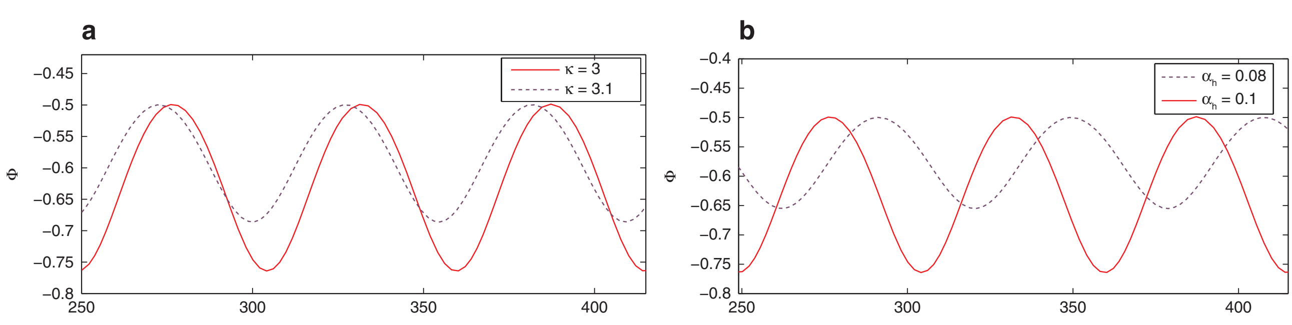

Figure 9: Effects of (a) κ and (b) α_h on NPIAW solution of the mKdV (20) with $\alpha_c = 1.1$, $f = 0.1$ and $V = 0.2$.

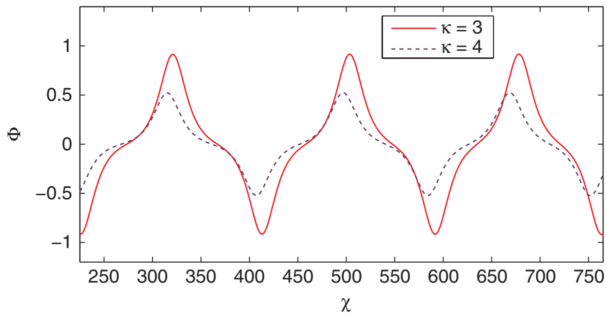

Figure 10: Effect of κ on SNPIAW solution for system (26) of the mKdV (20) with other system parametric data same as Figure 3.

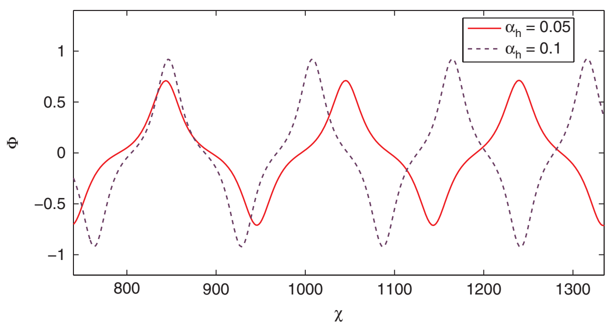

Figure 11: Effect of α_h on SNPIAW solution for system (26) of the mKdV (20) with system parameters same as Figure 3.

with parametric data same as Figure 3. We observe that amplitude and width of SNPIAWs are shortened when spectral index (κ) of electrons is increased.

In Figure 11, we present effect of α_h on small-amplitude SNPIAW solution of the mKdV (20) with system parametric data same as Figure 3. We observe from Figure 11 that when temperature of hot electrons is decreased, amplitude of small-amplitude SNPIAW flourishes while its width diminishes.

7 Conclusions

A multicomponent plasma constituting of cold fluid ions, κ-distributed hot and cold electrons has been considered. A small-amplitude IAW has been studied under the KdV and mKdV equations using RPT. Applying travelling wave transformation, the KdV and mKdV equations have been reduced to their corresponding dynamical systems (23) and (26). Using bifurcation theory of dynamical systems, all qualitative phase portrait profiles for dynamical systems (23) and (26) have been displayed. It has been observed from phase portrait profiles that $NHO_{1,0}$ and $NPO_{1,0}$ of dynamical system (23) obtained from the KdV equation (13) support IASW and NPIAW solutions, respectively. On the other hand, phase portrait profile consisting of $NHO_{1,0}$, $NPO_{1,0}$ and $SPO_{3,1}$ of dynamical system (26) obtained from the mKdV equation (20) supports IASW, NPIAW and SNPIAW solutions. Using bifurcation analysis through phase plane analysis, existence of small-amplitude SNPIAW solution of the mKdV equation in the considered plasma system has been reported for the first time. Furthermore, influences of spectral index (κ) and ratio (α_h) of effective temperature to hot electron temperature have been shown on compressive and rarefactive IASW, NPIAW and SNPIAW solutions of the mKdV equation (20). It has been observed that when temperature of hot electrons is low, small-amplitude SNPIAW flourishes. When spectral index of electrons approaches to Maxwellian limit, small-amplitude SNPIAW becomes more smooth. Therefore, our result shows existence of small-amplitude nonlinear and SNPIAWs in plasmas composing of κ-distributed cold and hot electrons. System parameters spectral index of electrons (κ) and temperature ratio (α_h) play key roles in bifurcation analysis of small-amplitude nonlinear and supernonlinear periodic ion-acoustic waves in superthermal plasmas.

Acknowledgement: Dr Asit Saha is thankful to SMIT and SMU for TMA Pai Research Grant (6100/SMIT/R&D/Project/05/2018). All authors are thankful to the reviewers and the editor for their comments and suggestions which helped to improve the paper.

References

[1] A. E. Dubinov, D. Y. Kolotkov, and M. A. Sazonkin, Plasma Phys. Rep. **38**, 833 (2012).
[2] A. E. Dubinov and D. Y. Kolotkov, IEEE Trans. Plasma Sci. **40**, 1429 (2012).
[3] A. E. Dubinov and D. Y. Kolotkov, High Energy Chem. **46**, 349 (2012).
[4] A. E. Dubinov and D. Y. Kolotkov, Plasma Phys. Rep. **38**, 909 (2012).
[5] F. Verheest, Phys. Plasma **16**, 013704 (2009).
[6] T. K. Baluku, M. A. Hellberg, and F. Verheest, EPL **91**, 15001 (2010).
[7] F. Verheest, Phys. Plasma **18**, 083701 (2011).
[8] A. Das, A. Bandyopadhyay, and K. P. Das, J. Plasma Phys. **78**, 149 (2012).
[9] F. Verheest, M. A. Hellberg, and I. Kourakis, Phys. Plasmas **20**, 082309 (2013).
[10] S. K. Maharaja, R. Bharuthram, S. V. Singh, and G. S. Lakhina, Phys. Plasmas **20**, 083705 (2013).
[11] F. Verheest, M. A. Hellberg, and I. Kourakis, Phys. Rev. **87**, 043107 (2013).
[12] O. R. Rufai, R. Bharuthram, S. V. Singh, and G. S. Lakhina, Phys. Plasmas **21**, 082304 (2014).
[13] S. A. El-Wakil, E. M. Abulwafa, and A A. Elhanbaly, Phys. Plasmas **24**, 073705 (2017).

[14] F. Verheest, M. A. Hellberg, and I. Kourakis, Phys. Plasmas **20**, 012302 (2013).
[15] C. P. Olivier, F. Verheest, and W. A. Hereman, Phys. Plasmas **25**, 032309 (2018).
[16] M. N. Ali, S. M. Husnine, A. Saha, S. K. Bhowmik, S. Dhawan, et al., Nonlinear Dyn. **94**, 1791 (2018).
[17] A. E. Dubinov and D. Y. Kolotkov, Rev. Mod. Plasma Phys. **2**, 2 (2018).
[18] T. Kamalam and S. S. Ghosh, Phys. Plasmas **25**, 122302 (2018).
[19] R. K. Dodd, J. C. Eilbeck, J. D. Gibbon, and H. C. Morries, Solitons Nonlinear Waves Equations, Academic Press Inc, London 1982.
[20] A. A. Mamun, Astrophys. Space Sci. **268**, 443 (1999).
[21] K. E. Lonngren, Opt. Quant. Electron. **30**, 615 (1998).
[22] A. Saha, P. Chatterjee, and C. S. Wong, Brazilian J. Phys. **45**, 656 (2015).
[23] W. F. El-Taibany and A. A. Mamun, Phys. Rev. E **85**, 026406 (2012).
[24] G. S. Lakhina, S. V. Singh, and A. P. Kakad, Phys. Plasmas **21**, 062311 (2014).
[25] A. Saha and P. Chatterjee, Eur. Phys. J. D **69**, 203 (2015).
[26] T. K. Maji, M. K. Ghorui, A. Saha, and P. Chatterjee, Brazilian J. Phys. 47, 295 (2017).
[27] A. Renyi, Acta Math. Hung. **6**, 285 (1955).
[28] V. M. Vasyliunas, J. Geophys. Res. **73**, 2839 (1968).
[29] P. Chatterjee, U. Ghosh, K. Roy, and S. V. Muniandy, Phys. Plasmas **17**, 122314 (2010).
[30] C. R. Choi, K. W. Min, and T. N. Rhee, Phys. Plasmas **18**, 092901 (2011).
[31] N. S. Saini, I. Kourakis, and M. A. Hellberg, Phys. Plasmas **16**, 062903 (2009).
[32] T. K. Baluku and M. A. Hellberg, Phys. Plasmas **15**, 123705 (2008).
[33] N. Ahmadihojatabad, H. Abbasi, and H. Hakimi Pajouh, Phys. Plasmas **17**, 112305 (2010).
[34] B. Sahu, Phys. Plasmas **17**, 122305 (2010).
[35] E. I. El-Awady, S. A. El-Tantawy, W. M. Moslem, and P. K. Shukla, Phys. Lett. A **374**, 3216 (2010).
[36] T. K. Das, S. Choudhury, A. Saha, and P. Chatterjee, J. Fizik Malayasia **38**, 010016 (2017).
[37] M. N. Kadijani, H. Abbasi, and H. H. Pajouh, Plasma Phys. Control Fusion **53**, 025004 (2011).
[38] I. Kourakis, S. Sultana, and M. A. Hellberg, Plasma Phys. Control Fusion **54**, 124001 (2012).
[39] S. H. Strogatz, Nonlinear Dynamics and Chaos, Westview Press, USA (2007).
[40] U. K. Samanta, A. Saha, and P. Chatterjee, Phys. Plasma **20**, 022111 (2013).
[41] O. R. Rufai, R. Bharuthram, S. V. Singh, and G. S. Lakhina, Adv. Spaces Res. **53**, 813 (2016).
[42] S. V. Singh and G. S. Lakhina, Commun. Nonlinear Sci. Numer. Simulat. **23**, 274 (2015).
[43] L. Mandi, A. Saha, and P. Chatterjee, Space Res. **64**, 427 (2019).
[44] A. Saha, N. Pal, and P. Chatterjee, Phys. Plasma **21**, 102101 (2014).
[45] M. M. Selim, A. El-Depsy, and E. F. El-Shamy, Astrophys. Space Sci. **360**, 66 (2015).
[46] A. Saha and J. Tamang, Adv. Space Res. **63**, 1596 (2019).
[47] J. Tamang and A. Saha, Zeitschrift für Naturforschung A **74**, 499 (2019).
[48] P. K. Prasad, S. Sarkar, A. Saha, and K. K. Mondal, Brazilian J. Phys. **49**, 698 (2019).
[49] F. Verheest, C. P. Olivier, and W. A. Hereman, J. Plasma Phys. **18**, 905820208 (2018).
[50] W. D. Jones, A. Lee, S. M. Gleman, and H. J. Doucet, Phys. Rev. Lett. **35**, 1349 (1975).
[51] T. E. Sheridan, M. J. Goeckner, and J. Goree, J. Vacuum Sci. Technol. A **9**, 688 (1991).
[52] S. N. Chow and J. K. Hale, Methods of Bifurcation Theory, Springer-Verlag, New York 1982.
[53] A. Saha, Commun. Nonlinear Sci. Numer. Simulat. **17**, 3539 (2012).
[54] J. Guckenheimer and P. J. Holmes, Nonlinear Oscillations, Dynamical Systems and Bifurcations of Vector Fields, Springer-Verlag, New York 1983.